Properties of Printer Calibration Targets

Davor Donevski, Diana Milčić, Jakov Borković

Keywords: G7, printer calibration, calibration target

Printer calibration targets can differ with respect to aims of the calibration. In this study, GrayFinder target as described in the G7 Specification was modified and tested on an RGB printer. It was inspected whether it is beneficial to vary all three device channels instead of keeping one channel constant. The relations between input value RGB ranges and CIE L*a*b* domain were also monitored. It was found that varying all channels can lead to improvement by widening L*a*b* domain, with the cost of increasing the target size.

1. Introduction

Device calibration generally has two aims: optimizing device performance and setting it to a known state. However, printing devices can be calibrated in different ways, depending on the aim of the calibration [1, 2]. Printer calibration methods can be divided into those that calibrate CMYK individually and those that calibrate it collectively [3]. In this study, the principles from the G7 Specification were applied. It prescribes the setting of the transfer curves depending on the device's tonal range and provides the gray balance definition. In addition to that, it specifies the tools used to achieve these aims. By the G7 calibration method, the transfer curves are modified in such a way to compress the dark tonal range in favor of preserving light tones. For devices with smaller tonal ranges, the compression is shifted toward lighter tones.

Gray balance, as defined by the G7 Specification, is a linear function of the substrate color. This means that CIE a* and b* values of the CMY step wedge patches converge from those of the unprinted substrate toward zero on the darkest patch. The tool used to achieve this, described in the G7 Specification, is known as the *GrayFinder Target*. It consists of the six groups of patches where the cyan is set at six different levels as an approximator of darkness. Within each of the six groups of patches, cyan is kept constant, while magenta and yellow are varied. By varying seven steps for M and Y, 49 patches within a group are obtained. This approach is very convenient for production presses where gray balance can be adjusted by both RIP curves and inking. Another tool, the *P2P target* can be used to calculate correction curves by using software [4]. However, the P2P target contains a relatively small number of near-neutral patches and a wide range of colors. For this reason, it is not able to achieve satisfactory results in all cases [5]. In order to obtain more accurate aim value predictions on a narrow range of near-neutral values, it is necessary to use a target adapted to this smaller domain. Various methods were developed to reduce the number of patches by selection of "optimal" sets on both calibration [6] and characterization targets [7, 8].

This study inspected the calibration accuracy achieved by using modified standard targets. Although it was conducted on a simple RGB desktop printer (device's driver receives RGB inputs and coverts them to colorant amounts, user having no direct control over them) with tools adapted to RGB device space, its nature is such that it similarly applies to CMYK devices.

2. Methodology

For the purpose of this study, four different targets were created and their performances tested on a desktop printer HP Deskjet 940c. The targets were printed on a plain 90g/m^2 paper and measured with X-Rite i1Pro spectrophotometer.

Prior to creating the targets, input R=G=B values which approximately correspond to aimed density values were determined. Values of GrayFinder target from G7 Specification were used. Central patches CMY triplets were inverted to account for inverse lightness exhibition of additive principle and scaled to 8-bit [0, 255] range. After printing and measuring L*a*b* values of those six patches, G7 NPDC curve was applied while using L* as an approximation of D. Having determined the required L* values, corresponding R=G=B triplets were determined using splines fitted to initial R=G=B, D values. These new values could now serve as central patches of targets. In addition to L*, aimed a* and b* values for the six central patches were determined according to G7 Specification, as a linear function of substrate color converging to zero at the darkest patch (R=G=B=0).

With known R=G=B triplets of the six central patches, targets could now be created. Table 1 displays specifics of the four targets created and tested in this study.

Table 1: Tested targets

TARGET	# patches	Varying channels	Varying range / # steps
A	294	G and B	±9 / 3
B	1350	G and B	±21 / 7
C	750	R, G and B	±4 / 2
D	750	R, G and B	±10 / 2

Targets A and B were created on a principle similar to GrayFinder target. Within each of the six groups of patches, R channel is kept at fixed value, and G and B are varied. Targets A and B differ in range of varying G and B channel. Target A had narrower range and 7x7 patches in each of the six groups. Target B had 15x15 patches in each of the six groups and was hence much larger. Targets C and D were created on a different principle of varying all three RGB channels as it was expected that this should result in wider L*a*b* domain for narrower RGB varying ranges, as well as more accurate model predictions resulting from more even RGB values distribution. As varying all three channels results in a larger number of permutations than varying only two, number of steps was decreased to keep the target size (number of patches) reasonable. The difference between targets C and D is in range width of varying RGB values.

In order to determine RGB input values required to achieve aimed L*a*b* values, targets were fitted with a third order polynomial model of the following form, here presented in more common forward model representation:

$$[L^*a^*b^*] = [1\ \ R\ \ G\ \ B\ \ RG\ \ RB\ \ GB\ \ R^2\ \ G^2\ \ B^2\ \ R^2G\ \ R^2B\ \ G^2B\ \ G^2R\ \ B^2R\ \ B^2G\ \ RGB\ \ R^3\ \ G^3\ \ B^3]\ A$$

Table 2: Target A domain

INPUT	DOMAIN			AIM		
RGB	L*	a*	b*	L*	a*	b*
113	43.20	-7.76	-18.96	46.25	0.07	-0.24
	47.35	4.96	-3.05			
151	56.66	-8.41	-21.07	57.19	0.28	-0.98
	62.50	4.27	-5.30			
174	66.75	-5.19	-20.14	66.14	0.76	-2.62
	70.08	3.81	-7.99			
190	71.00	-5.10	-21.81	73.60	1.52	-5.22
	75.06	5.36	-8.25			
208	76.20	-4.90	-22.48	80.07	2.42	-8.32
	81.10	5.64	-8.78			
234	82.92	-3.32	-20.32	87.03	3.24	-11.11
	89.39	5.53	-9.90			

Its performances on four different targets were evaluated using the training value set (not the independent data set) as only comparison between targets was required.

3. Results

Tables 2 to 5 display L*a*b* minimum and maximum values for each of the six groups of patches on targets A, B, C and D. The values were obtained by printing and measuring targets with a spectrophotometer.

Table 2 displays L*a*b* ranges for target A. As it can be seen, L* and a* values are satisfactory as aimed values fall within chart ranges, except for the L* value on the third patch which falls outside, but is fairly close to range's lower boundary. However, almost all aimed b* values fall outside the ranges, and most of them are quite far from the range's upper boundary. Figure 1 shows the convex hull of the set of points from target A (blue) and aimed values (red). It is clear that all aims fall outside the convex hull of the points from target A.

Table 3 displays L*a*b* ranges for target B. As it can be seen, all of the L*a*b* aimed values of all six patches are falling within target's ranges. This was arrived to intentionally by widening the RGB input range. Figure 2 shows the convex hull of the set of points from target B (blue) and aimed values (red). It is clearly visible that although the aims fell within the ranges, that does not mean that they fall within the convex hull of a set of points included in the target.

Table 3: Target B domain

INPUT	DOMAIN			AIM		
RGB	L*	a*	b*	L*	a*	b*
113	41.26	-18.59	-28.26	46.25	0.07	-0.24
	52.82	12.43	8.72			
151	52.61	-14.76	-29.05	57.19	0.28	-0.98
	64.07	11.99	7.27			
174	63.00	-12.86	-29.45	66.14	0.76	-2.62
	72.34	11.17	5.97			
190	68.45	-11.35	-27.73	73.60	1.52	-5.22
	77.67	9.60	1.13			
208	72.79	-10.45	-25.99	80.07	2.42	-8.32
	83.49	9.73	0.41			
234	77.87	-6.83	-22.81	87.03	3.24	-11.11
	89.29	9.28	-1.62			

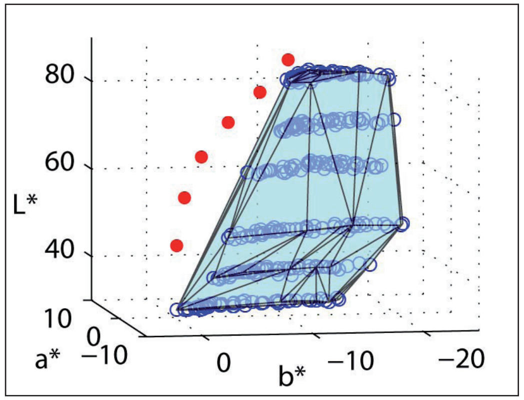

Figure 1: Target A values distribution

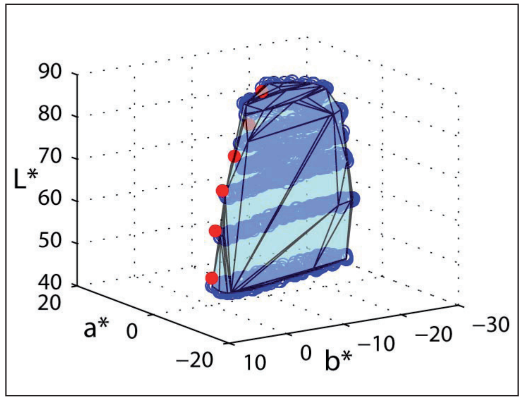

Figure 2: Target B values distribution

Table 4 displays L*a*b* ranges for target C. As it can be seen, similarly to target A, L* value of the third patch and all b* values fall outside the target ranges. What's more, if we compare target's C to target's A ranges, it can be noted that target's C ranges are somewhat narrower. It was expected that varying all three values would widen the ranges. However, it must be taken into consideration that input RGB ranges of target C were less than half of target A's RGB ranges, and L*a*b* ranges on target C were not even close to being halved. Figure 3 shows the convex hull of the set of points from target C (blue) and aimed values (red). It is visible that the aims fall quite far away from the convex hull for darker target patches, but the lightest aim fell within it. Compared to target A, although the input RGB ranges of target C were much narrower, and therefore insufficient to include aims in darker tones (which require more correction as they are linearly scaled towards a*=0, b*=0), varying all three channels led to more favorable distribution of points in L*a*b* space which resulted in including the lightest aim within the convex hull of target's C set of points.

Table 5 displays L*a*b* ranges for target D. As it can be seen, aimed b* values of third and fourth patch do not fall within the target's ranges. Compared to target C, target D had wider RGB input ranges and managed to include four patches' b* values, but two were still left out. The RGB input range of target D was only slightly wider than range of target A, and yet it managed to include most of the aimed values within its L*a*b* ranges, unlike target A which did not include any b* value. This confirms that varying all three channels provides wider

Table 4: Target C domain

INPUT	DOMAIN			AIM		
RGB	L*	a*	b*	L*	a*	b*
113	43.93	-3.37	-16.98	46.25	0.07	-0.24
	46.87	5.14	-7.51			
151	56.92	-3.55	-17.91	57.19	0.28	-0.98
	62.17	6.10	-8.55			
174	67.02	-0.74	-16.91	66.14	0.76	-2.62
	70.90	5.99	-9.60			
190	71.72	-1.06	-15.97	73.60	1.52	-5.22
	74.74	5.10	-9.92			
208	76.79	-2.23	-18.54	80.07	2.42	-8.32
	80.39	5.88	-9.95			
234	85.48	-0.42	-16.31	87.03	3.24	-11.11
	89.46	5.27	-10.91			

Table 5: Target D domain

INPUT	DOMAIN			AIM		
RGB	L*	a*	b*	L*	a*	b*
113	41.98	-12.95	-21.4	46.25	0.07	-0.24
	47.90	9.46	-0.10			
151	54.47	-13.72	-24.29	57.19	0.28	-0.98
	64.35	11.29	1.27			
174	64.76	-9.19	-23.80	66.14	0.76	-2.62
	71.73	8.29	-3.97			
190	69.51	-7.37	-22.45	73.60	1.52	-5.22
	76.08	8.72	-6.49			
208	74.71	-8.37	-23.94	80.07	2.42	-8.32
	81.98	9.63	-6.15			
234	81.02	-7.01	-21.99	87.03	3.24	-11.11
	90.87	8.96	-6.41			

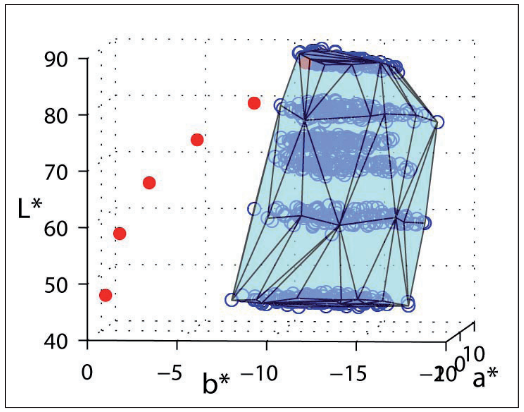

Figure 3: Target C values distribution

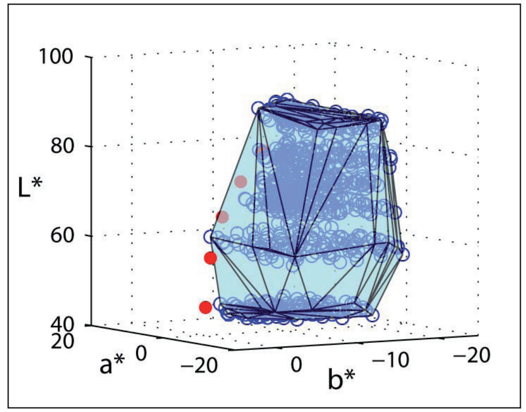

Figure 4: Target D values distribution

L*a*b* ranges than when only two channels are varied by the same amount. Figure 4 shows the convex hull of the set of points from target D (blue) and aimed values (red). It is visible that only two darkest aims were not contained within the convex hull of target's D set of points. Compared to target B, target D's input RGB ranges were halved and target's size (number of patches) was almost halved (Table 1). In spite of this, varying all three channels led to relatively wider L*a*b* ranges and more favorable distribution of target's points in L*a*b* space, which led to including most (except the two darkest) aims within the convex hull of target's D set of points.

Tables 6, 8, 10 and 12 display aimed L*a*b* values, their corresponding inputs predicted by a third order polynomial model and measured L*a*b* values on targets A to D. Tables 7, 9, 11 and 13 display model performance on targets A to D.

As can be seen from Table 6 and figures 5a and 5b, L* values were predicted with fair accuracy, while a* values

Table 6: Target A predicted inputs and measured responses

AIM			PREDICTED			MEASURED		
L*	a*	b*	R	G	B	L*	a*	b*
46.25	0.07	-0.24	121	104	76	46.00	1.70	4.30
57.19	0.27	-0.98	158	138	106	58.40	1.80	8.70
66.14	0.76	-2.62	181	165	135	66.50	1.20	4.90
73.60	1.52	-5.22	198	187	165	73.60	1.70	-4.20
80.07	2.42	-8.32	214	209	195	79.80	0.70	-8.50
87.03	3.24	-11.11	234	231	225	87.80	1.90	-10.90

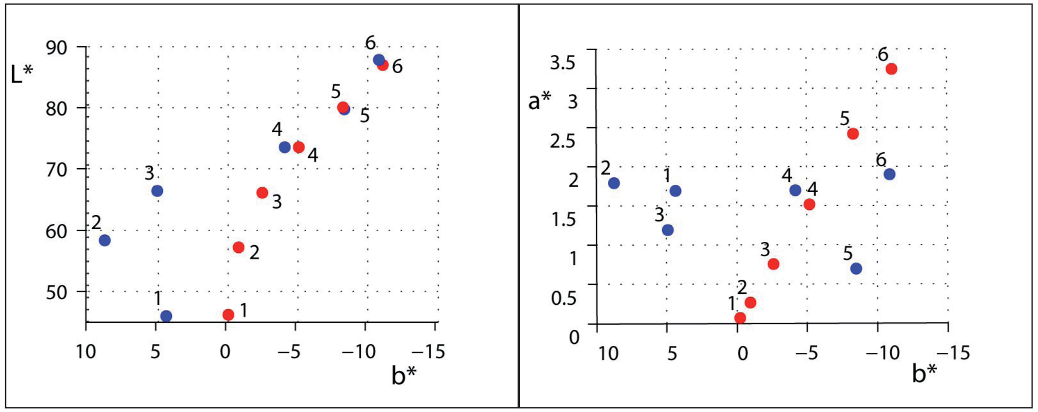

Figure 5: Aim and measured values, target A

Table 7: Model performance on target A

N	min	median	mean	max
294	0.14	0.79	0.86	2.16

were "evened out", i.e. not linearly decreasing and b* values deviate from aimed considerably. The extent of b* values deviation was such that these patches exhibited a clearly visible yellow cast. Table 7 displays the model performance on target A patches. The model performance is quite satisfactory, and the results of b* values prediction are not. The reason for this is that Table 7 displays model performance on the target A values, i.e. the same values used to determine the model parameters. If we used the independent data set within the model domain, the performance would be slightly worse, but still satisfactory. However, as stated previously for results in Table 2, aimed b* values do not fall within model's domain (Figure 1, aims (red) outside the convex hull). Extrapolation led to significant errors in prediction.

As can be seen from Table 8 and figures 6a and 6b, widening the domain led to significant improvement. L* values were predicted with fair accuracy. As for a* values, although they are not perfectly linear, improvement in their accuracy is considerable. The b* values also

Table 8: Target B predicted inputs and measured responses

AIM			PREDICTED			MEASURED		
L*	a*	b*	R	G	B	L*	a*	b*
46.25	0.07	-0.24	124	114	102	48.00	0.40	-2.60
57.19	0.27	-0.98	155	143	130	59.70	1.10	-2.80
66.14	0.76	-2.62	177	166	151	67.50	1.10	-4.80
73.60	1.52	-5.22	197	187	173	73.20	2.10	-7.70
80.07	2.42	-8.32	216	208	198	79.90	2.10	-10.00
87.03	3.24	-11.11	240	233	228	88.70	3.40	-11.30

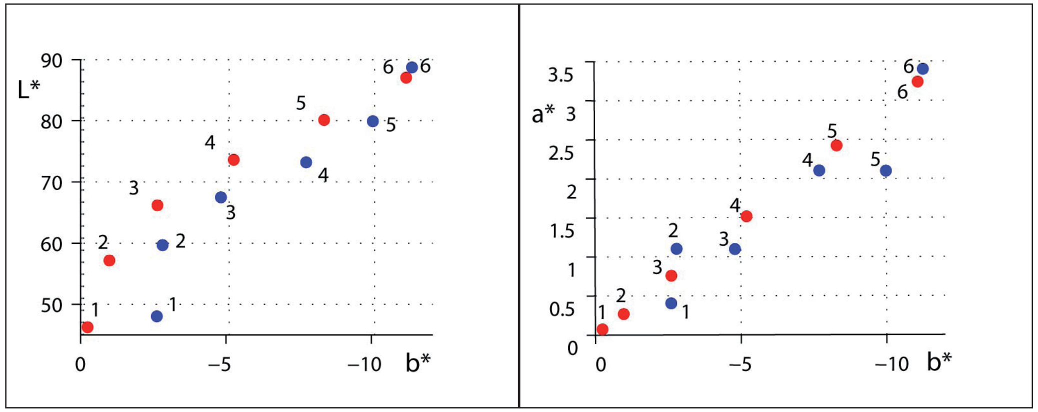

Figure 6: Aim and measured values, target B

Table 9: Model performance on target B

N	min	median	mean	max
1350	0.11	1.11	1.21	3.63

deviate from aimed to some extent and are not perfectly linear, but are fairly accurate. From Table 9 it can be seen that widening the domain led to somewhat poorer model performance. However, it was neccesary in order to fit the aimed b* values within the model's domain. Although in this case the aims didn't fall within the convex hull (model's domain), getting it close to them led to significant improvements in predicting RGB inputs required to achieve L*a*b* aimed values as extrapolation was smaller.

As can be seen from tables 10 and 11, and figures 7a and 7b, the performance of target C was rather poor. The reason for this was that the chosen input RGB value range was too narrow, leading to much too small L*a*b* domain (Figure 3). It can be noted how L* values of darker patches deviate from aims to a larger extent as the aims are quite far outside the convex hull. The maximum model error of 5,37 was not expected on such a small domain, apart from that the error central tendency measures are rather small as expected.

Table 10: Target C predicted inputs and measured responses

AIM			PREDICTED			MEASURED		
L*	a*	b*	R	G	B	L*	a*	b*
46.25	0.07	-0.24	124	114	102	48.00	0.40	-2.60
57.19	0.27	-0.98	155	143	130	59.70	1.10	-2.80
66.14	0.76	-2.62	177	166	151	67.50	1.10	-4.80
73.60	1.52	-5.22	197	187	173	73.20	2.10	-7.70
80.07	2.42	-8.32	216	208	198	79.90	2.10	-10.00
87.03	3.24	-11.11	240	233	228	88.70	3.40	-11.30

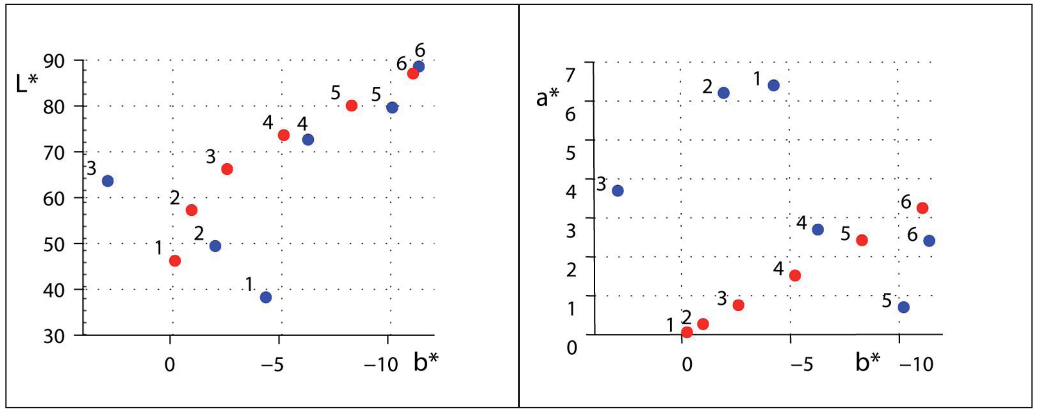

Figure 7: Aim and measured values, target C

Table 11: Model performance on target C

N	min	median	mean	max
750	0.07	0.84	0.98	5.37

As can be seen from tables 12 and 13, and figures 8a and 8b, target D performance was similar to that of target B. Some poorer performance is visible in the linearity of a* values. However, the target D was considerably smaller than target B and its domain was relatively large.

To summarize, figures 1-4 reveal that regardless of varying two or all three channels, varying them in both directions to the same extent (Table 1) for a given target results in obtaining values centered around substrate's a* and b*. As the aim of calibration as specified by G7 Specification is to have a* and b* linearly scaled towards zero on a scale from light to dark tones, this approach is ineffective. Standard targets use it as they have to accomodate a variety of different substrates that might be used (bluish, yellowish). To suceed in that and fit the aims within the target's convex hull, they have to set device input RGB (or, in the case of P2P target MY) ranges wide. This results in that a lot of the points are sampled from regions of L*a*b* space which are distant from aims and are of no interest. In addition to that, when using color transformation model, a lot of its prediction power is wasted on those uninteresting regions, reducing its accuracy in regions around aims.

Table 12: Target D predicted inputs and measured responses

AIM			PREDICTED			MEASURED		
L*	a*	b*	R	G	B	L*	a*	b*
46.25	0.07	-0.24	125	116	101	48.60	-1.70	-1.30
57.19	0.27	-0.98	154	143	129	59.30	1.50	-1.70
66.14	0.76	-2.62	178	167	151	67.50	1.80	-5.00
73.60	1.52	-5.22	198	190	174	74.40	0.90	-7.10
80.07	2.42	-8.32	216	210	200	80.10	1.40	-10.80
87.03	3.24	-11.11	238	232	228	88.50	3.30	-11.90

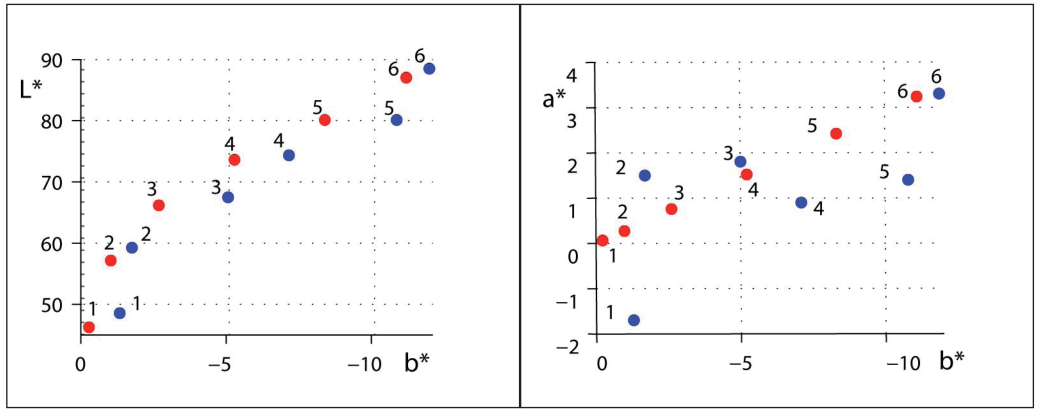

Figure 8: Aim and measured values, target D

Table 13: Model performance on target D

N	min	median	mean	max
750	0.07	1.11	1.17	3.84

4. Conclusion

This study has shown how calibration target design affects calibration accuracy. As a general rule, the target should be defined on as small domain as possible, but still including aimed values. It should be somewhat wider, i.e. not contain aimed values on the boundary as boundary values are known to be less accurately predicted by models [9]. In addition to that, larger target (more patches) usually results in greater accuracy. It was shown how the use of standard targets can lead to less than satisfactory results. Varying all channels is beneficial as it results in more favorable L*a*b* values distribution. Our future work will concentrate on the development of a method of determining device domain and generation of a target optimized for a particular device.

5. References

[1] Fraser, B./Murphy, C./Bunting, F. (2005): "Real World Color Management", 2nd ed., Peachpit Press, Berkeley, CA.
[2] Sharma, G. (2003): "Digital Color Imaging Handbook", CRC Press, Boca Raton.
[3] Craig, D.C., Wang, S. (2008): "Color Calibration Optimization", NIP24 - Digital Fabrication 2008, 24th International Conference on Digital Printing Technologies, Pittsburgh, PA, 611-615.
[4] The G7 Specification 2008, IdeAlliance, 2008.
[5] Juric, I./Karlovic, I./Tomic, I. (2012): "The possibility of using G7 method for calibration and characterization of Xerox Docucolor", The 6. International GRID symposium 2012, Novi Sad, Serbia.
[6] Kuo, Y./Chiu, G./Yih, Y./Allebach, J. (2011): "Calibration color patch reduction for digital electrophotography, NIP27 - Digital Fabrication 2011, 27th International Conference on Digital Printing Technologies, Minneapolis, MN.
[7] Mahy, M. (2000): "Analysis of color targets for output characterization", IS&T/SID 8th CIC, Scottsdale.
[8] Cheung, T./Westland, S. (2004): "Color selections for characterization charts", CGIV2004, Aachen.
[9] Green, P./MacDonald, L. (2002): "Colour Engineering", John Wiley and Sons Ltd, Chichester, UK.

(received for the first time: 28-09-12)

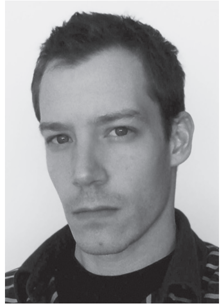

Davor Donevski
Dr. Sc.,
Faculty of Graphic Arts,
University of Zagreb,
Croatia

davor.donevski@grf.hr

Diana Milčić
Prof., Dr. Sc.,
Faculty of Graphic Arts,
University of Zagreb,
Croatia

diana.milcic@grf.hr

Jakov Borković
Dipl. Ing.,
Alterpress d.o.o.,
Zagreb,
Croatia

jakov.borkovic@alterpress.hr